COMPARATIVE EVALUATION OF ELECTRON AND GAMMA INDUCED EFFECTS ON FBG FABRICATED IN STANDARD AND RADIATION HARDENED OPTICAL FIBERS BY DIFFERENT TECHNIQUES

Razvan MIHALCEA[1], Daniel IGHIGEANU[2], Daniel NEGUT[3], Andrei STANCALIE[1*]

Gamma and electrons radiation induced effects on FBG written in standard and radiation hardened optical fibers by different fabrication methods are discussed. Four FBG are exposed to the two radiation types up to 120kGy while their response is recorded in real time. Radiation tolerance of all components is reported with respect to RIA while BWS from 10pm up to 120pm proves dependent on fiber type, radiation and fabrication method. Results lead to special discussion on the protection coatings on the gratings region as these may influence electron radiation induced effects as opposite from gamma-ray, where presumably this element is not impacting the radiation induced spectral changes.

Keywords: fiber Bragg gratings, radiation sensing, gamma radiation, electron radiation

1. Introduction

Optical fibers have been studied for many decades, becoming part of an increasing number of industries, telecommunication having of course the largest demand. Aside, optical fibers applications are more or less trivially found in fields such as automotive[1], oil and gas industry[2], structural health monitoring [3] or biosensing [4],[5],[6].

Optical fiber-based technology has found wide interest for applications in radiation environments [7] due to several factors. Mainly, the most appealing among these are the *immunity* to electromagnetic fields*, real time remote* interrogation over long distances, the *small size* of the optical components (down to 1 mm length and 125

[1] [1]Center for Advanced Laser Technologies, National Institute for Laser, Plasma and Radiation Physics, 409 Atomistilor St., RO-077125 Magurele, Romania
[2]Accelerators Department, National Institute for Laser, Plasma and Radiation Physics, 409 Atomistilor St., RO-077125 Magurele, Romania
[3]"Horia Hulubei" National Institute for R&D in Physics and Nuclear Engineering, 30 Reactorului St., RO-077125 Magurele, Romania

micrometer width) and the possibility to tailor the proposed solution to *best fit* the application. Research widens towards interdisciplinary applications such as space exploration, aerospace, high energy physics, defense industry, nuclear installations [8], and medical diagnostics [9].

Exploring and customizing novel optical fiber-based platforms for ionizing radiation diagnostics, sensing, energy distribution or for developing *radiation hardened* devices is certainly appealing especially due to the technological progress of the fabrication techniques. A wide range of sensors developed, starting from custom fiber Bragg gratings (FBG) - UV or fs-laser written [10], long period gratings (LPG) fabricated in single mode (SM) optical fibers doped/co-doped with different materials in core/cladding region [11], or even fiber-laser based [12] are the subject of several research groups worldwide. These devices, demonstrated their potential to retrieve and feed-back real time information from harsh environments, independently [13], [14] or forming matrixes by multiplexing several gratings [15].

While testing optical fiber sensors in ionizing radiation, the ambition is to target a) radiation tolerance up to high accumulated dose, b) to set a dose rate dependence and c) enhancing sensitivity up to lowest dose rate such as Gy level, currently found in medical applications.

In the current work, we discuss in a comparative manner the effect of two different ionizing radiation types, namely 60-CO gamma ray and electrons obtained by a linear accelerator, on fiber Bragg gratings fabricated by two techniques. We aim in providing vital analyses based on experimental data which can lead to a FBG-based hybrid sensing system. Furthermore we demonstrate its functionality up to high radiation total accumulated dose with the possibility of double-compensation: radiation or temperature.

2. Materials and methods

2.1 Optical platforms

For the current work and with respect to several advantages, the optical fibers chosen were of single-mode type and divided to standard Ge-doped and pure silica core fiber. Considered for sensing mechanisms, the gratings fabricated were of FBG type. Since these structures are well studied and characterized for decades from the point of view of the physical mechanism, we only briefly stress the main features, considered as influencing the current experimental work, as follows:

FBG work as selective filters attributed to a periodic modulation of the optical fibers core's refractive index. While part of the emitted spectra is further transmitted,

a specific resonant wavelength, λ_{Bragg} gets reflected by the structure with respect to the effective refractive index (n_{eff}) and the modulation period (Λ):

$$\lambda_{Bragg} = 2n_{eff}\Lambda \quad (1)$$

A linear temperature dependence of an FBG is following:

$$\lambda_{Bragg} = \lambda_{Bragg}(T0) + \alpha_0(T - T_0) \quad (2)$$

Where, α_0 shows the sensors' temperature sensitivity, meaning the variation of the resonance wavelength along with induced temperature. Although mechanical strain dependent, FBG sensors in the current work were mechanical stress free therefore being not vital to insist on the mechanical induced changes components within the spectral characterization.

2.2 Materials and methods:

The most common and standard fabrication method of FBG is the exposure of Ge-doped silica fibers to high photonic energy UV light [16]. In order to have the inscription process possible the photosensitivity of the material needs enhancement. Therefore doping with high concentration of Ge in the core region is required. However, the presence of Ge-content, makes the fiber platforms more vulnerable to high energy ionizing radiation. The FBG fabrication methods can be divided into linear absorption methods using continues-wave UV lasers and nonlinear absorption methods using ultra short pulse lasers such as the femtosecond (fs) lasers. On the other hand, the fs laser inscriptions are performed with a different mechanism, the multiphoton absorption, in which case the photosensitivity of the fiber is not mandatory. The fs inscribed gratings have several advantages when compared to UV gratings such as: better tensile tolerance, the inscription can be performed through the different coatings, higher temperature stability and survivability [17-20].

In the current scenario, the fibers configuration included two commercial Ge-doped optical fibers each containing FBG, fabricated by UV exposure, of 10cm length with a trivial temperature sensitivity of 10pm/1^{o}C. Secondly, two additional gratings were custom femtosecond lased fabricated by Loptek GmbH (Berlin, Germany) in pure silica core fiber, bend insensitive. The fiber's type was FIBERCORE SM1500SC having 7 cm core diameter and standard 125 micrometer core plus cladding diameter. The operating wavelength of both fiber types is 1550nm with a cut-off wavelength between 1400nm and 1500nm. For the SM1500SC the numerical aperture is ~0.18 while the attenuation is less than 0.7 db/k, at 1550nm. Finally the coating diameter is of 245 μm, although not particularly of importance in such experiments but in the

current case may be leading to a discussion following the results section. In the case of the pure silica core fiber, the gratings surface was coated with acrylate while in the case of the FBG written in standard Ge-doped fibers, the region containing the grating was uncoated due to fabrication method.

2.3. Experimental setup

Three main experimental setups are being utilized for the dedicated spectral characterization as follows.

a) A Laboratory setup at CETAL department part of INFLPR is optimised for temperature calibration of the optic components and includes both heating chambers and interrogation equipment. A temperature chamber (Memmert, GmbH) was controlled to induce temperature shift up to 80^{o}C while all FBG were carefully placed in the central part of the chamber. Temperature was increased from room temperature with a 5^{o} degree step and a fixed slope in order to prevent sudden changes and to favor homogeneity. The resonance (Bragg) wavelength shift was recorded in real time while temperature was measured with a calibrated Type J thermocouple placed near the gratings. A second temperature sensor was fixed and part of the T-chamber. Spectral acquisition was provided in all cases by an optical interrogator type LUNA SM125 equipped with four acquisition channels. The four gratings were not multiplexed but interrogated separately using four standard single mode fiber connections, each independently connected to a separate channel. Following, a brief schematic of the setup as well as calibration results are presented, where FBG1 and FBG2 are UV fabricated respectively FBG3 and FBG4 are fs-laser inscribed and further referenced with these abbreviations:

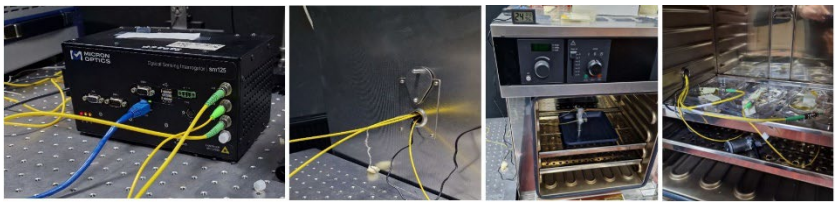

Fig.1. Temperature calibration setup

FBG1	9.8 pm/1^{o}c
FBG2	9.6 pm/1^{o}c
FBG3	10 pm/1^{o}c
FBG4	10.2 pm/1^{o}c

Table 1
BWS(pm) vs. T(^{o}C)

b) Gamma irradiation setup

The gamma-ray irradiation was performed at IRASM department, part of the "Horia Hulubei" National Institute of Physics and Nuclear Engineering, A customized gamma chamber was utilized to expose the gratings to a 60-Co source. The setup was developed and utilized extensively in other works for the real time investigations of optical fibers sensors [21], being particularly described in [22]. Briefly we stress the fact that this irradiation setup induces homogeneously gamma-radiation in a 5000 cm space, the sensors being placed in a particular position in such way that the dosimetry is well known and monitored. The temperature profile is recorded in real time grace to several adaptations of the gamma chamber, respectively by introducing two J-type thermocouples within two gas channels, while connection fibers are crossed in two additional channels. Optical interrogator is placed a few meters near the gamma chamber keeping transmission loss to a minimum due to short distance connection fibers. Adaptors are kept outside the 5000 cm irradiation space together with the single mode connection fibers to avoid additional radiation induced attenuation outside the gratings region. This dedicated setup was subject of many comparative studies and its performance in terms of stability and reproducibility is well checked periodically. Dosimetry is being performed during exposure, in the sensors region with traceable elements. Fig.2 shows a schematic of the gamma-irradiation setup:

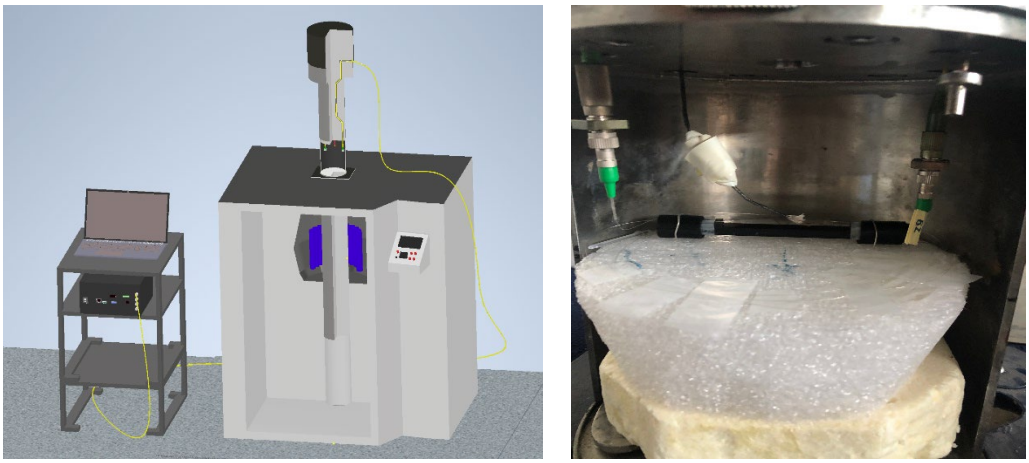

Fig.2 Gamma irradiation setup

c) Electron irradiation setup

The electron irradiation was performed at the Electron Accelerators Laboratory, National Institute for Laser, Plasma and Radiation Physics. Having several previous works describing the setup [23][24][25], we only emphasize the essentials: A

"travelling-wave" linear accelerator, driven by a 2MW peak power tunable EEV M5125 type magnetron operating in the S-band (2992-3001 MHz) is utilized to irradiate the samples up to 120 kGy, respectively an electron energy of 5.5 MeV. The two samples are irradiated in open space, while connecting fibers 20 m long reach outside the radiation area up to the interrogation unit. The same optical interrogator is utilized in all setups for reproducibility purpose. While exposed, the Bragg wavelength is recorded with 1 second acquisition rate, together with the full spectral shape of the investigated sensors, respectively FBG2 and FBG4, but with lower frequency of 300s. Together with spectral characteristics, a thermocouple 15m long is placed inside the irradiation area of 10 cm radius. Both the sensors and thermocouple are situated at 40 cm under the initial beam exit and are centered in the mentioned diameter. Total accumulated dose was of 120 kGy for an exposure of 30 minutes. All peripherals are kept outside radiation zone. An experimental schematic diagram is found bellow in Fig. 3:

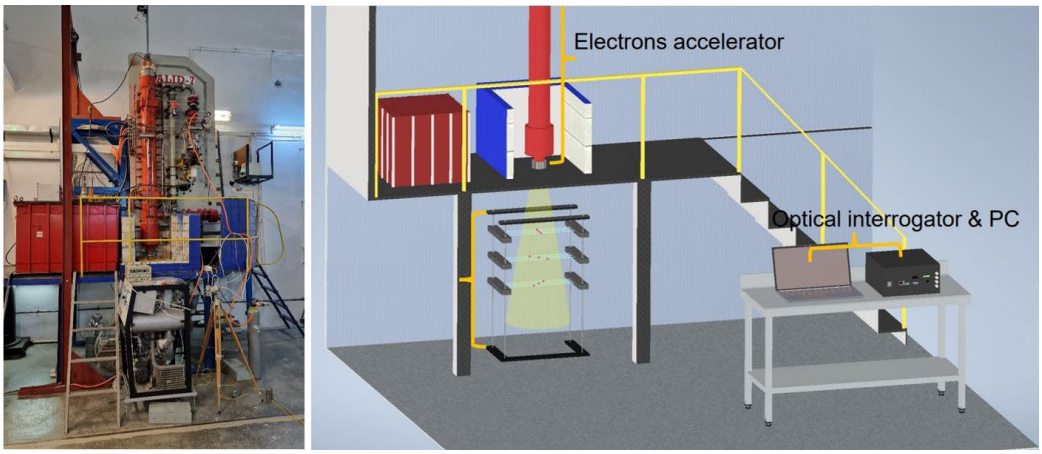

Fig. 3. Electron irradiation setup

3. Results

3.1 Exposure of the FBG to 60-Co Gamma radiation

Two FBG, respectively FBG1 and FBG3 from above description, were placed inside the gamma chamber and centered in the 5000cm^3 space. The J-type thermocouple was fixed at ~1 cm on top of the gratings and the chamber was set to 22 hours irradiation time while the dose rate is stable at the value of 2.45 kGy/h. The spectral characteristics of both gratings were recorded in real time, both in the case of transmission spectra between 1510nm-1590nm and the Bragg wavelengths, further referred as λ_{B1} and λ_{B2}. Spectral print of both gratings, as recorded prior and after the exposure to γ-ray are presented in figure 4. It is important to stress that temperature

variation influence on the Bragg wavelength shift (BWS) was not subtracted in Fig.4, since we first wish to present the original recorded data so to emphasize on the influence of this (T) physical parameter.

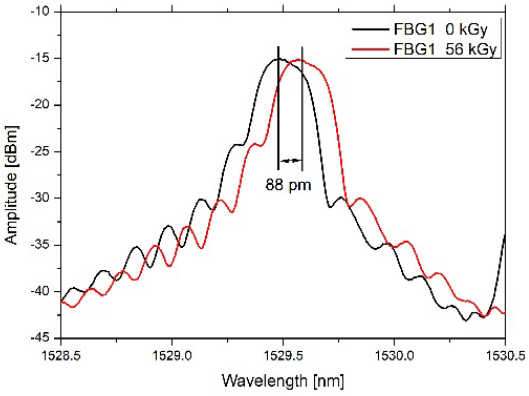

Fig.4 a) FBG1 (UV) before and after γ exposure

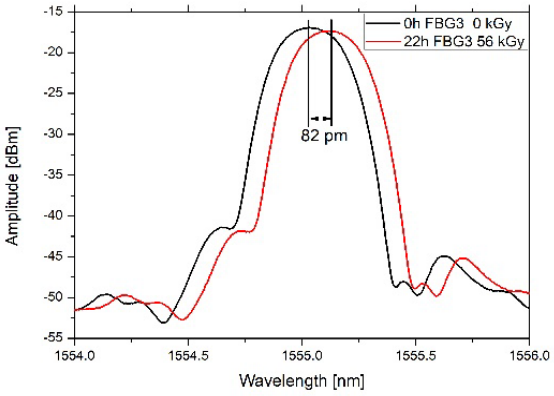

Fig.4 b) FBG3 (fs-laser) before and after γ exposure

The BWS recorded in real time is further presented in figure 5 while temperature profile recorded during the exposure can be observed in Fig.6. Following the reported temperature coefficients calculated during the laboratory calibration stage, and the uniformity of the temperature inside the gamma chamber, the T correction was possible and further applied to bring the adjustments to the Bragg wavelengths, therefore reporting the genuine data of the γ influence on the optical sensors:

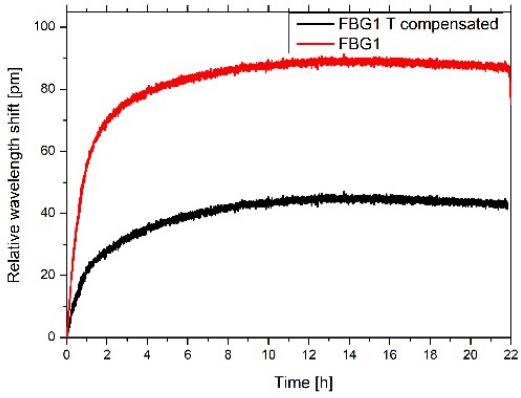

Fig.5 a) Temperature compensated BWS recorded for FBG1

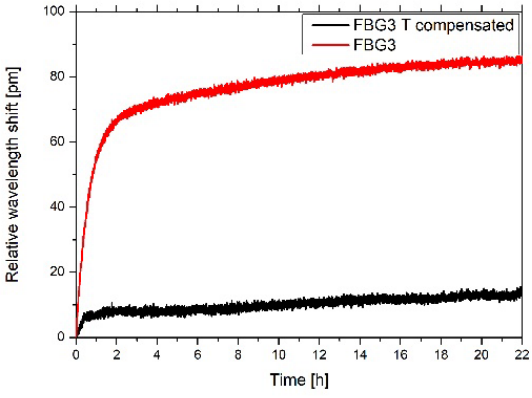

Fig.5 b) Temperature compensated BWS recorded for FBG3

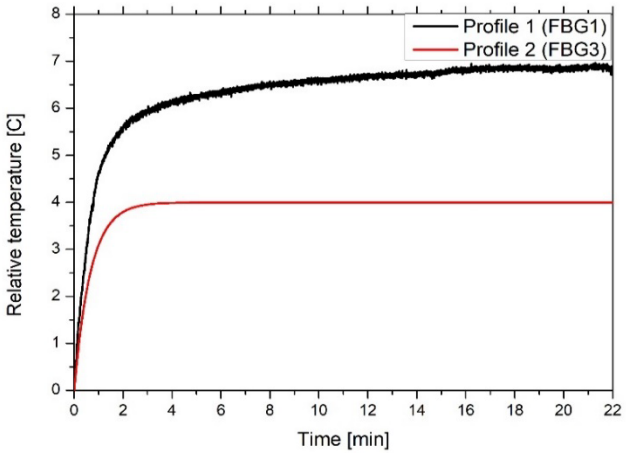

Fig.6 Temperature profiles for FBG1 (black) and FBG3 irradiation (red)

3.2 Electron radiation effects on standard UV fabricated and fs-laser written FBG

As different from the two gamma experiments described above, the FBG pair, identical from the fabrication point of view with the previous ones, was subjected to *e*-beam simultaneously. The setup is described in section 2.3, the total accumulated dose being of 120 kGy while having a uniform dose-rate of 3.8 kGy/min. In a comparative manner with the 3.1 section, the spectral changes recorded are represented bellow in the following figures.

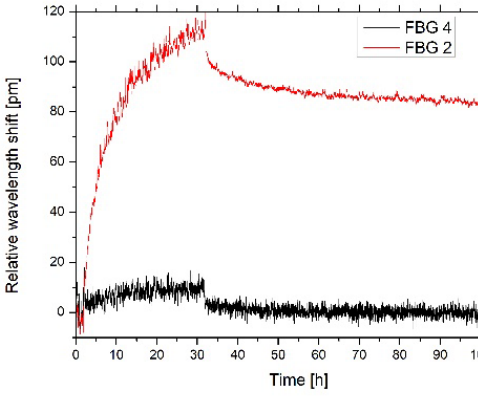

Fig.7 BWS induced by e-beam for FBG2 and FBG4

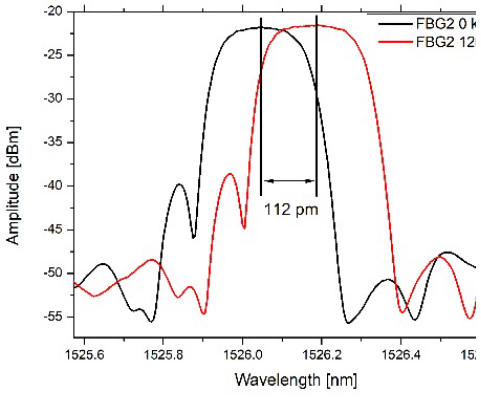

Fig.8 Transmission spectra of FBG2 and FBG4 before and after e-beam exposure

Worth to be noticed, Fig.6 presents both induced spectral changes during irradiation in real time as well the variation of the resonance wavelengths following irradiation for about 80 minutes. Easily noticeable, the FBG2, although presenting an obvious recovery tendency blue shifting towards the initial value, the impact of electron radiation is clearly visible after the beam is shut down. The temperature variation recorded with the thermocouple placed inside the beam is reported in Fig.9.

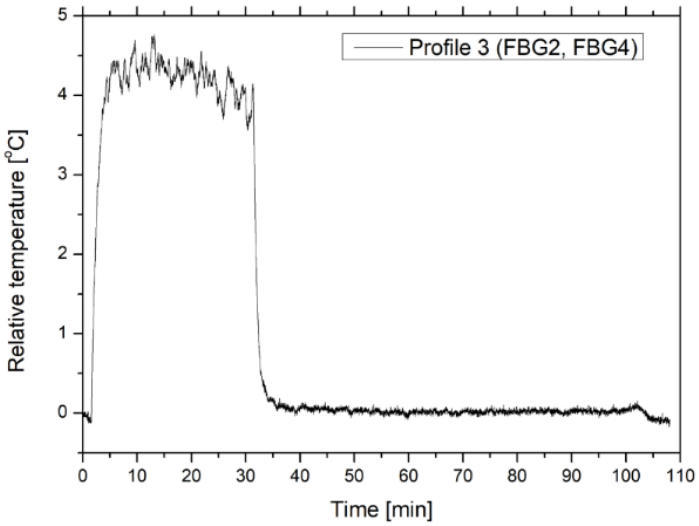

Fig.9 Temperature profile of the electron irradiation

4. Discussions and conclusions

In the light of the above mentioned results, there are several discussions necessary to approach. To briefly summarize, the real time response of the four FBG is represented in the figure 10 with respect to the Bragg wavelength induced variation during radiation exposure for the first 110 minutes. Temperature changes induced during the experiments were recorded along with spectral data provided by the sensors, again in real time. Accumulated radiation dose is different depending on each experiment. Electrons energy is different than CO-60, therefore a more detailed comparison following same experimental conditions is not trivial and this parameter needs to be taken into account.

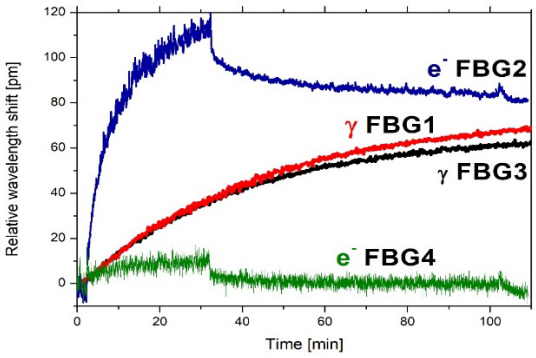

Fig. 10

We need to emphasize on the following remarks. The FBG sensors were stress free during all experiments. Therefore, the mechanical influence on the BWS is negligible. Radiation induced attenuation (RIA) is the main and most important radiation induced effect on optical fibers and their degradation in harsh environments. However, in the current case, for the mentioned dose and parameters, and as demonstrated in Fig.4 and Fig.8, RIA is limited and may be considered negligible in both gamma and electron irradiation experiments. This is attributed to the optical fibers type and dopant concentration if any but also to the fact that within the setup, only very short part of the fiber, containing the gratings, was directly exposed, the rest being shielded along with the peripherals (e.g. splices, adaptors). Taking into account the above considerations, the changes of the Bragg wavelengths is clearly representative as radiation induced change and makes the subject of the current work being directed correlated with radiation effects on the gratings. A summary of the approximate BWS during exposure is found in Table 2, including temperature corrections for gamma experiment.

`Table 2.

Results summary

Sensor No.	Fiber type	Fabrication method	Radiation type	Accumulated dose	Dose rate	BWS
FBG1	Ge-doped	Phase-mask	Gamma	56 kGy	2,45kGy/h	40pm
FBG2	Ge-doped	Phase-mask	Electrons	120 kGy	228kGy/h	120pm
FBG3	Pure silica	Fs-laser	Gamma	56 kGy	2,45kGy/h	10pm
FBG4	Pure silica	Fs-laser	electrons	120 kGy	228kGy/h	10 pm

Special discussion needs to be carried out based on the temperature calibration and radiation effects especially in the case of the e-beam exposure. As mentioned in earlier section, all the four gratings have a similar temperature sensitivity of about 10pm/^{o}C. If, during gamma exposure temperature influence can be clearly separated from radiation one, given the saturation level of the BWS and the recorded temperature in the gratings region thus making the data coherent and sound, during the electron irradiation the subtraction of T effect was not possible since sensors data is not in agreement with irradiation time and temperature measured by the thermocouple. As seen in the Fig.9, representing the temperature profile of roughly 30 minutes of irradiation, the temperature gets stabilized in the first five minutes, and should represent a induced shift of about 40 pm based only on thermo-optic coefficients. If in the case of FBG 2, the effect may be a component of the total represented shift, in the case of the FBG4 written in pure silica core fiber considered radiation tolerant, the 40 pm shift does not exist. Since FBG 4 host fiber has similar thermo-optic coefficient, demonstrated in the calibration stage by the FBG peak variation, linear with temperature in the controlled chamber, and having a BWS of precisely 10.2 pm/1^{o}C, the electrons induced temperature change should be visible as well on the same optical sensor. The difference may be due, and coming back to 2.2 section, to the acrylate coating found on FBG4 but not on FBG2. However these effects need to be further investigated by replicating similar experiments with different coated FBG written in pure silica core fibers.

Acknowledgement

This work was supported by the UEFISCDI project PED 666/2022 "MEMOIR". The research was partially supported by Romanian Ministry of Research, Innovation and Digitalization under Romanian National Core Program LAPLAS VII – contract no. 30N/2023.

REFERENCES

[1] *Beguni, C.; Căilean, A.-M.; Avătămăniței, S.-A.; Zadobrischi, E.; Stoler, R.; Dimian, M.; Popa, V.; Béchadergue, B.; Chassagne, L.* In-Vehicle Visible Light Communications Data Transmission System Using Optical Fiber Distributed Light: Implementation and Experimental Evaluation. Sensors 2022, **22**, 6738. https://doi.org/10.3390/s22186738

[2] *Christopher Baldwin*, Fiber Optic Sensors in the Oil and Gas Industry: Current and Future Applications, Opto-Mechanical Fiber Optic Sensors, Pages 211-236, 2018 https://doi.org/10.1016/B978-0-12-803131-5.00008-8

[3] *U.M.N. Jayawickrema, H.M.C.M. Herath, N.K. Hettiarachchi, H.P. Sooriyaarachchi, J.A. Epaarachchi*,Fibre-optic sensor and deep learning-based structural health monitoring systems for civil structures: A review,Measurement,Volume **199**,2022,111543,ISSN 0263-2241, https://doi.org/10.1016/j.measurement.2022.111543

[4] *Flavio Esposito, Lucia Sansone, Anubhav Srivastava, Angela Maria Cusano, Stefania Campopiano, Michele Giordano, Agostino Iadicicco*, Label-free detection of vitamin D by optical biosensing based on long period fiber grating, Sensors and Actuators B: Chemical,Volume **347**, 2021, 130637, ISSN 0925-4005, https://doi.org/10.1016/j.snb.2021.130637

[5] *Li, B.; Zhang, R.; Bi, R.; Olivo, M.* Applications of Optical Fiber in Label-Free Biosensors and Bioimaging: A Review. Biosensors 2023, 13, **64**. https://doi.org/10.3390/bios13010064

[6] *F. Esposito, A. Srivastava, L. Sansone, M. Giordano, S. Campopiano and A. Iadicicco,* "Label-Free Biosensors Based on Long Period Fiber Gratings: A Review," in IEEE Sensors Journal, vol. **21,** no. 11, pp. 12692-12705, 1 June1, 2021, https://doi.org/10.1109/JSEN.2020.3025488

[7] *Zhang J, Xiang Y, Wang C, Chen Y, Tjin SC, Wei L.* Recent Advances in Optical Fiber Enabled Radiation Sensors. Sensors (Basel). 2022 Feb 1;**22**(3):1126. PMID: 35161870; PMCID: PMC8840197, https://doi.org/10.3390/s22031126

[8] *Stancălie, A., Esposito, F., Ranjan, R.* et al. Arc-induced Long Period Gratings in standard and speciality optical fibers under mixed neutron-gamma irradiation. Sci Rep 7, **15845** (2017), https://doi.org/10.1038/s41598-017-16225-4

[9] *A. Giaz, M. Galoppo, N. Ampilogov, S. Cometti, J. Hanly, O. Houlihan, W. Kam, M. Martyn, O. Mc. Laughlin, R. Santoro, G. Workman, M. Caccia, S. O'Keeffe*, ORIGIN, an EU project targeting real-time 3D dose imaging and source localization in brachytherapy: Commissioning and first results of a 16-sensor prototype, Nuclear Instruments and Methods in Physics Research Section A: Accelerators, Spectrometers, Detectors and Associated Equipment, Volume **1048**, 2023, 167999, ISSN 0168-9002, https://doi.org/10.1016/j.nima.2022.167999

[10] *Theodosiou, A.; Leal-Junior, A.; Marques, C.; Frizera, A.; Fernandes, A.J.S.; Stancalie, A.; Ioannou, A.; Ighigeanu, D.; Mihalcea, R.; Negut, C.D.; Kalli, K.* Comparative Study of γ- and e-Radiation-Induced Effects on FBGs Using Different Femtosecond Laser Inscription Methods. Sensors 2021, **21**, 8379. https://doi.org/10.3390/s21248379

[11] *Andrei Stăncălie, Dan Sporea, Daniel Neguț, Flavio Esposito, Rajeev Ranjan, Stefania Campopiano, Agostino Iadicicco*, Long Period Gratings in unconventional fibers for possible use as radiation dosimeter in high-dose applications,Sensors and Actuators A: Physical,Volume **271**,2018,Pages 223-229,ISSN 0924-4247, https://doi.org/10.1016/j.sna.2018.01.034.

[12] *Perez-Herrera, R.A.; Stancalie, A.; Cabezudo, P.; Sporea, D.; Neguț, D.; Lopez-Amo, M.* Gamma Radiation-Induced Effects over an Optical Fiber Laser: Towards New Sensing Applications. Sensors 2020, **20**, 3017. https://doi.org/10.3390/s20113017

[13] *Flavio Esposito, Andrei Stăncălie, Constantin-Daniel Neguţ, Stefania Campopiano, Dan Sporea, and Agostino Iadicicco,* "Comparative Investigation of Gamma Radiation Effects on Long Period Gratings and Optical Power in Different Optical Fibers," J. Lightwave Technol. **37**, 4560-4566 (2019)

[14] *Esposito, F., Ranjan, R., Stăncălie, A.* et al. Real-time analysis of arc-induced Long Period Gratings under gamma irradiation. Sci Rep **7**, 43389 (2017). https://doi.org/10.1038/srep43389

[15] *Sporea, D.; Stăncălie, A.; Becherescu, N.; Becker, M.*; Rothhardt, M. An Electron Beam Profile Instrument Based on FBGs. Sensors 2014, **14**, 15786-15801. https://doi.org/10.3390/s140915786

[16] *Smelser, C.W.; Mihailov, S.J.; Grobnic, D.* Formation of Type I-IR and Type II-IR gratings with an ultrafast IR laser and a phase mask. Opt. Express. 2005, **13**, 5377–5386, doi:10.1364/OPEX.13.005377

[17] *Theodosiou, A.; Lacraz, A.; Polis, M.; Kalli, K.; Tsangari, M.; Stassis, A.; Komodromos, M.* Modified fs-Laser Inscribed FBG Array for Rapid Mode Shape Capture of Free-Free Vibrating Beams. IEEE Photonics Technol. Lett. 2016, **28**, 1509–1512.

[18] *Theodosiou, A.; Lacraz, A.; Stassis, A.; Koutsides, C.; Komodromos, M.; Kalli, K*. Plane-by-Plane Femtosecond Laser Inscription Method for Single-Peak Bragg Gratings in Multimode CYTOP Polymer Optical Fiber. J. Light. Technol. 2017, **35**, 5404–5410.

[19] *Theodosiou, A.; Fokine, M.; Hawkins, T.; Ballato, J.; Gibson, U.J.; Kalli, K*. Characterisation of silicon fibre Bragg grating in near-infrared band for strain and temperature sensing. Electron. Lett. 2018, **54**, 1393–1395.

[20] *Theodosiou, A.; Aubrecht, J.; Peterka, P.; Kalli, K.* Femtosecond laser plane-by-plane Bragg gratings for monolithic Thulium-doped fibre laser operating at 1970 nm. In Micro-Structured and Specialty Optical Fibres VI; SPIE—The International Society for Optical Engineering: Bellingham, WA, USA, 2019; Volume **11029**

[21] *F. Esposito et al*., "The impact of gamma irradiation on optical fibers identified using Long Period Gratings," in Journal of Lightwave Technology, 2022 (early access), https://doi.org/JLT.2022.3191163

[22] *Stancalie, A.; Esposito, F.; Neguț, C.D.; Ghena, M.; Mihalcea, R.; Srivastava, A.; Campopiano, S.; Iadicicco*, A. A New Setup for Real-Time Investigations of Optical Fiber Sensors Subjected to Gamma-Rays: Case Study on Long Period Gratings. Sensors 2020, **20**, 4129. https://doi.org/10.3390/s20154129

[23] *Haifeng Qi* et al 2021 J. Phys.: Conf. Ser. **2112** 012005 DOI 10.1088/1742-6596/2112/1/012005
[24] *Chen, Y., Li, J., Wang, Z.* et al. Quantitative Measurement of γ-Ray and e-Beam Effects on Fiber Rayleigh Scattering Coefficient. Photonic Sens **11**, 298–304 (2021). https://doi.org/10.1007/s13320-020-0580-7
[25] *Desheng Fan, Yanhua Luo, Binbin Yan, Andrei Stancălie, Daniel Ighigeanu, Daniel Neguţ, Dan Sporea, Jianzhong Zhang, Jianxiang Wen, Jiajun Ma, Pengfei Lu, and Gang-Ding Peng,* "Ionizing Radiation Effect upon Er/Yb Co-Doped Fibre Made by In-Situ Nano Solution Doping," J. Lightwave Technol. **38**, 6334-6344 (2020)